

# Chemical Science

Volume 12  
Number 5  
7 February 2021  
Pages 1571–1946

rsc.li/chemical-science



ISSN 2041-6539

**EDGE ARTICLE**

Agustí Lledós, Salvador Conejero *et al.*  
Reversible carbon-boron bond formation at platinum  
centers through  $\sigma$ -BH complexes

Cite this: *Chem. Sci.*, 2021, 12, 1647

All publication charges for this article have been paid for by the Royal Society of Chemistry

# Reversible carbon–boron bond formation at platinum centers through $\sigma$ -BH complexes†

Pablo Ríos,<sup>a</sup> Rocío Martín-de la Calle,<sup>a</sup> Pietro Vidossich,<sup>b</sup> Francisco José Fernández-de-Córdova,<sup>a</sup> Agustí Lledós<sup>\*c</sup> and Salvador Conejero<sup>†\*a</sup>

A reversible carbon–boron bond formation has been observed in the reaction of the coordinatively unsaturated, cyclometalated, Pt(II) complex [Pt(I<sup>t</sup>Bu<sup>i</sup>Pr')(I<sup>t</sup>Bu<sup>i</sup>Pr)][BAr<sup>F</sup>], **1**, with tricoordinated boranes HBR<sub>2</sub>. X-ray diffraction studies provided structural snapshots of the sequence of reactions involved in the process. At low temperature, we observed the initial formation of the unprecedented  $\sigma$ -BH complexes [Pt(HBR<sub>2</sub>)(I<sup>t</sup>Bu<sup>i</sup>Pr')(I<sup>t</sup>Bu<sup>i</sup>Pr)] [BAr<sup>F</sup>], one of which has been isolated. From –15 to +10 °C, the  $\sigma$ -BH species undergo a carbon–boron coupling process leading to the platinum hydride derivative [Pt(H)(I<sup>t</sup>Bu<sup>i</sup>Pr–BR<sub>2</sub>)(I<sup>t</sup>Bu<sup>i</sup>Pr)] [BAr<sup>F</sup>], **4**. Surprisingly, these compounds are thermally unstable undergoing carbon–boron bond cleavage at room temperature that results in the 14-electron Pt(II) boryl species [Pt(BR<sub>2</sub>)(I<sup>t</sup>Bu<sup>i</sup>Pr)<sub>2</sub>] [BAr<sup>F</sup>], **2**. This unusual reaction process has been corroborated by computational methods, which indicate that the carbon–boron coupling products **4** are formed under kinetic control whereas the platinum boryl species **2**, arising from competitive C–H bond coupling, are thermodynamically more stable. These findings provide valuable information about the factors governing productive carbon–boron coupling reactions at transition metal centers.

Received 6th October 2020  
Accepted 9th November 2020

DOI: 10.1039/d0sc05522k

rsc.li/chemical-science

## 1. Introduction

The formation of C–B bonds, mediated by transition metal complexes, has become an important tool for the synthesis of organoboron compounds,<sup>1</sup> an important family of organic molecules in synthetic organic chemistry and in materials science.<sup>2</sup> From the mechanistic point of view, there have been several reports that point to the participation of  $\sigma$ -BH ( $\sigma$ -borane) complexes as key intermediates in the formation of the carbon–boron bonds in metal-alkyl or -aryl compounds. For example, Hartwig *et al.* have shown, by means of DFT calculations, that  $\sigma$ -BH complexes of rhodium and tungsten are transient species in the borylation of alkanes, where the driving force is the formation of the C–B bonds (Scheme 1).<sup>3</sup>

Although most of this type of C–H borylation processes have been carried out using rhodium and iridium systems,<sup>4</sup> there

have been a few reports on the utilization of platinum complexes for the formation of C–B bonds, either in stoichiometric reactions or in catalytic processes.<sup>5</sup> Turculet and Stradiotto reported the dehydrogenative coupling of B–H/C–H bonds at a Pt(II) center,<sup>5a</sup> whereas Chatani, Tobisu *et al.* suggested the participation of  $\sigma$ -BH complexes in the platinum-catalyzed borylation of arenes.<sup>5b,c</sup> However, the interaction of tricoordinated hydroboranes with platinum centers leading to  $\sigma$ -BH complexes has proven elusive.<sup>6</sup> In addition, examples of transition metal  $\sigma$ -borane alkyl complexes [M(R)(HBR<sub>2</sub>)] are extremely rare, and those that have been isolated did not show further reactivity involving the formation of carbon–boron bonds.<sup>7</sup> Isolation of this type of compounds might offer an invaluable opportunity for determining the factors that can lead



Scheme 1  $\sigma$ -BH complexes proposed as intermediates in the borylation of C–H bonds of alkanes reported by Hartwig *et al.*<sup>3</sup>

<sup>a</sup>Instituto de Investigaciones Químicas (IIQ), Departamento de Química Inorgánica, CSIC and Universidad de Sevilla, Centro de Innovación en Química Avanzada (ORFEO-CINQA), C/ Américo Vespucio 49, Sevilla, 41092, Spain. E-mail: sconejero@iiq.csic.es

<sup>b</sup>Molecular Modeling & Drug Discovery Laboratory, Istituto Italiano di Tecnologia, Via Morego 30, 16163 Genoa, Italy

<sup>c</sup>Departament de Química, Universitat Autònoma de Barcelona, Edifici Cn, Cerdanyola del Vallès, 08193, Spain. E-mail: agusti@klingon.uab.es

† Electronic supplementary information (ESI) available: Experimental details, spectroscopic, computational data (PDF). X-ray crystallographic data (CIF). Cartesian coordinates of the selected DFT optimized structures (XYZ). CCDC 2033931–2033934. For ESI and crystallographic data in CIF or other electronic format see DOI: 10.1039/d0sc05522k





{<sup>1</sup>H} NMR: 18.6 ppm). All these sigma complexes are stable at temperatures ranging from  $-15$  to  $+10$  °C, with complex **3c** being the most stable. In line with these findings, DFT calculations estimate favorable  $\Delta G$  of formation at  $-30$  °C of  $-2.3$ ,  $-0.6$  and  $-3.1$  kcal mol<sup>-1</sup> for **3a**, **3b** and **3c**, respectively (see Fig. S33 in the ESI†).

The increased thermal stability of complex **3c** has allowed us to obtain crystals suitable for X-ray diffraction analysis by slow diffusion of CH<sub>2</sub>Cl<sub>2</sub> solution into pentane at  $-25$  °C (Fig. 2). The platinum center is found in a nearly planar environment, with two NHCs and one  $-\text{CH}_2-$  unit occupying three coordination sites and the B–H moiety the fourth. The angle defined by atoms C13–Pt1–H1 and Pt1–H1–B1 are  $168.5(1)^\circ$  and  $105(2)^\circ$ , respectively, very close to those observed in the related  $\sigma$ -SiH derivative [Pt(HSiEt<sub>3</sub>)(<sup>t</sup>Bu<sup>1</sup>Pr′)(<sup>t</sup>Bu<sup>1</sup>Pr)] [BAR<sup>F</sup>] ( $173.1(1)^\circ$  and  $103(2)^\circ$ ).<sup>9</sup> The Pt1–H1 and H1–B1 bond distances are 1.69(4) Å and 1.19(3) Å, respectively. The latter is slightly elongated with respect to the B–H bond of boranes<sup>13</sup> and comparable to related  $\sigma$ -BH primary aminoborane complexes.<sup>14</sup> The Pt1⋯B1 distance of 2.31 Å is considerably larger than the sum of covalent radii (2.2 Å), suggesting that, if any, the interaction between these two atoms is weak.<sup>15</sup> In fact, topological analysis of the electron density and its laplacian (see ESI†) revealed the presence of bond critical points (BCPs) between Pt and H, and H and B, yet no BCP between Pt and B was observed.<sup>16</sup> This fact suggests that the coordination mode is better described as  $\eta^1$ -BH instead of the common  $\eta^2$ -BH mode reported for other transition metals.<sup>6,13,17</sup> Bonding interactions were further analyzed in terms of localized orbitals.<sup>18</sup> The centroid of the localized orbital corresponding to the B–H bond ( $X_{\text{BH}}$ , Fig. 3) is close to the H center, in agreement with a marked hydride character of this H atom, and is displaced from the B–H axis towards Pt, indicative of a perturbed sigma bond. At the same time, one Pt centroid ( $X_{\text{Pt}}$ ) is slightly moved away (0.431 Å) from the nucleus, compared to the other Pt centroids (0.345–0.398 Å), and pointing to B. We have previously characterized similar interactions in cationic Pt(II)  $\sigma$ -silane complexes, which adopt a rare  $\eta^1$ -SiH coordination mode.<sup>9</sup>

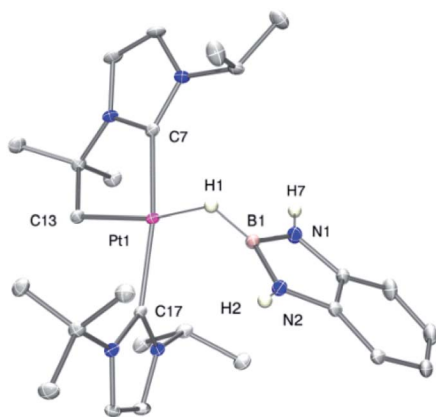


Fig. 2 Molecular structure of the cationic component as determined by X-ray diffraction of complex **3c** (ellipsoids at 30% probability). Selected bond distances (Å) and angles (°): Pt1–H1, 1.69(4); H1–B1, 1.19(3), Pt1–C13, 2.054(2); Pt1–H1–B1, 105(2); C13–Pt1–H1, 168.5(1).

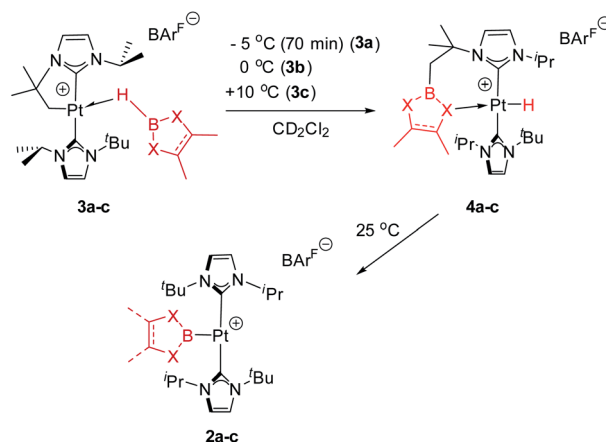


Fig. 3 Localized orbital analysis of **3c**. The molecular structure is overlaid with the centroids of the localized orbitals (small green dots). Dotted lines highlight the Pt–B and Pt–H distances.

As in the previously characterized  $\eta^1$ -SiH platinum complexes,<sup>9</sup> the coordination of the  $\sigma$ -bonded ligand is very flexible. We computed the energetic cost of deforming the Pt–H–B angle in **3c** (see Table S4 and Fig. S40†). Starting from the energy minimum at  $101.6^\circ$ , closing the angle to  $78^\circ$  or opening it to  $154^\circ$  requires less than 6 kcal mol<sup>-1</sup>. More acute angles ( $68^\circ$ ) lead to borane dissociation instead of B–H bond cleavage, which contrasts with what was observed between **1** and hydrosilanes, for which closing the Pt–H–Si angle led ultimately to the Si–H oxidative addition.<sup>9</sup> Importantly, QTAIM analysis did not reveal any BCP between Pt and B in structures with acute Pt–H–B angles (Fig. S38 and S39†).

### 2.3 Thermal evolution of $\sigma$ -BH Pt(II) complexes: reversible C–B coupling en route to boryl complexes

As mentioned before complexes **3a–c** are only marginally thermally stable, and upon warming at temperatures above  $-15$  °C (**3a**),  $0$  °C (**3b**) or  $+10$  °C (**3c**) undergo a rearrangement that involves the cleavage of the B–H bond and the formation of a new C–B bond leading to complexes **4a–c** (Scheme 4). The reaction is particularly clean in the case of complex **3a**, for



Scheme 4 Rearrangement of complexes **3a–c**.







Fig. 6 Gibbs energy profile in dichloromethane for the C–B (green trace) and C–H (red trace) bond formation pathways (NHCs in *cis*) upon reaction between **1** and HBpin. Gibbs energies at 298 K in kcal mol<sup>-1</sup>. The Gibbs energy of **1** + HBpin has been taken as zero-energy.

7.8 kcal mol<sup>-1</sup> (TS1). However, going back from **4a** to **3a-cis** requires an activation of only 22.4 kcal mol<sup>-1</sup>, which can be provided raising enough the temperature. At 25 °C transition state TS4 (22.1 kcal mol<sup>-1</sup>) can be overcome and the reaction is driven by the formation of the most stable product, **2a** (thermodynamic control). The boryl complex **2a** is formed *via* a C–H coupling process. The rationalization for the experimental observations combines the C–B (Fig. 6, green trace) and C–H (Fig. 6, red trace) bond formation pathways: at low temperatures, C–B bond formation takes place through the aforementioned described mechanism, yielding **4a**. Then, increasing the temperature to 25 °C allows the system to undergo the reverse pathway, reaching **3a-cis** and, after a conformational change, **3a-cis'**, which initiates the C–H coupling pathway leading to the most stable product **2a**. The different energetic barriers observed from **3a-cis** and **3a-cis'** leading to C–B or C–H coupling, respectively, might have (at least in part) a steric origin. The orientation of the pinacol substituents in **3a-cis'** is likely inducing some steric repulsions with the spectator NHC ligand in *cis* to it, and this might account for the different Pt...B bond distances (0.13 Å) observed in both **3a-cis** and **3a-cis'**. Reducing the steric effects on the borane might reduce the energy differences. In fact, as stated before, in the reaction carried out with HBcat, complexes **4b** and **2b** coexist in a certain range of temperatures, suggesting that, in this case, formation of C–B and C–H bonds have very similar energetic barriers.

### 2.5 Electronic analysis of C–B and C–H coupling processes

Exploration of the potential energy surface of **1** + HBpin system has allowed disclosing the mechanism for the formation of C–B

and C–H coupling products and their interconversion. Calculations have shown that rupture of B–H and H<sub>2</sub>C–Pt bonds and formation of either C–B and Pt–H or C–H and Pt–B bonds entail similar energy requirements. To reveal these bonding rearrangements we applied a localized orbital approach, which turned highly useful to analyze other organometallic reactions.<sup>18</sup> In this approach Kohn–Sham molecular orbitals are transformed into maximally localized orbitals (LMOs) and the centroids of these LMOs are computed for selected structures along the reaction path. The movement of the LMOs centroids along the reaction describes the electronic rearrangements taking place in the bond-breaking and bond-forming processes. In this way an arrow-pushing description of the C–B and C–H coupling processes can be obtained from DFT calculations. Recently, we applied this approach to analyze C–Si bond coupling reactions.<sup>19</sup>

Fig. 7 shows the relevant LMOs together with their centroids in three representative structures of the key chemical step of each process. The corresponding arrow-pushing schemes are also depicted in Fig. 7. The same LMOs are involved in both processes, one describing the H<sub>2</sub>C–Pt bond and another corresponding to the B–H bond. Similarly to **3c**, in the initial structures **3a-cis** and **3a-cis'** the centroid of the B–H bond is displaced and very close to the H center, pointing to the hydride character of this atom. In the formation of the C–H bond the centroid of the C–Pt bond moves from the C–Pt axis to the C–H axis, while the centroid of the B–H bond moves from the B–H axis to the B–Pt axis. This corresponds to a sigma-CAM type reaction,<sup>26</sup> in which, formally, a proton is being transferred to the methylene fragment and a boryl





Fig. 7 C–H (top) and C–B (bottom) bond forming events from the analysis of the movements of the centroids of the localized orbitals, represented by small purple dots. Isosurfaces of the localized orbitals involved in the bond-breaking/bond-forming processes are also shown. For each process the deduced arrow-pushing scheme is also shown.

moiety is being formed. Conversely, in the formation of the C–B bond the centroid of the C–Pt bond moves from the C–Pt axis to the B–C axis, while the centroid of the B–H bond moves from the B–H axis to the H–Pt axis (again, a sigma-CAM rearrangement). Formally, a borinium<sup>27</sup> is being transferred to the methylene fragment and a metal-hydride is being formed. Therefore, the possibility to generate both boryl and borinium species from a platinum  $\sigma$ -BH complex is the underlying reason that allows both C–B and C–H bond coupling processes to take place in this system.

### 3. Conclusion

The low-electron count Pt(II) complex  $[\text{Pt}(\text{I}^t\text{Bu}^i\text{Pr})(\text{I}^t\text{Bu}^i\text{Pr})][\text{BAR}^F]$ , **1**, reacts with tri-coordinated boranes in a set of reactions that start with formation of  $\sigma$ -BH complexes, **3**, in which the interaction of the B–H fragment with the cationic platinum center adopts a rare  $\eta^1$ -BH coordination mode. These species evolve, as a function of temperature, by either formation of hydride complexes  $[\text{Pt}(\text{H})(\text{I}^t\text{Bu}^i\text{Pr}-\text{BR}_2)(\text{I}^t\text{Bu}^i\text{Pr})][\text{BAR}^F]$ , **4**, or platinum boryl derivatives  $[\text{Pt}(\text{BR}_2)(\text{I}^t\text{Bu}^i\text{Pr})_2][\text{BAR}^F]$ , **2**. We were able to detect species **3**, **4** and **2** by means of low temperature



NMR spectroscopy and, in some cases, by X-ray diffraction, providing snapshots of this unusual reactivity. DFT-based analyses support  $\sigma$ -complex assisted metathesis mechanisms ( $\sigma$ -CAM),<sup>26</sup> preceded by *trans* to *cis* isomerization of the NHC ligands. These calculations indicate that carbon-boron coupling products are energetically more accessible and that the competitive process leading to C–H bond coupling is more energy demanding. However, as the temperature increases, the thermodynamic stability of the final products determines the formation of the C–H bond coupling products. Steric effects between the substituents at the boryl fragment and the spectator NHC ligand in complexes **3a-cis** and **3a-cis'** might be behind the different energetic barriers. These results contribute to the mechanistic understanding of the factors that can lead to productive borylation and advance the design of new effective catalytic systems for such reactions.

## Conflicts of interest

There are no conflicts to declare.

## Acknowledgements

Financial support (FEDER contribution) from the MINECO (Projects CTQ2016-76267-P, CTQ2017-87889-P, PID2019-109312GB-I00 and RED2018-102387-T), the CSIC (AEPP-CTQ2016-76267-P) and the use of computational facilities of the Supercomputing Center of Galicia (CESGA) is gratefully acknowledged. P. R. thanks the Junta de Andalucía for a research grant.

## Notes and references

- (a) J. V. Obligacion and P. J. Chirik, *Nat. Rev. Chem.*, 2018, **2**, 15–34; (b) M. Oestreich, E. Hartmann and M. Mewald, *Chem. Rev.*, 2013, **113**, 402–441; (c) I. Beletskaya and C. Moberg, *Chem. Rev.*, 2006, **106**, 2320–2354; (d) T. Ishiyama and N. Miyaura, *Chem. Rev.*, 2004, **3**, 271–280; (e) K. Burgess and M. J. Ohlmeyer, *Chem. Rev.*, 1991, **91**, 1179–1191; (f) T. B. Marder and N. C. Norman, *Topics in Catal.*, ed. W. Leitner and D. G. Blackmond, Baltzer Science Publishers, Amsterdam, 1998, vol. 5, pp. 63–73.
- (a) *Synthesis and Applications of Organoboron Compounds*, in *Topics in Organometallic Chemistry*, ed. E. Fernández and A. Whiting, Springer, Heidelberg, 2015; (b) *Boronic acids: preparation and applications in organic synthesis, medicine and materials*, ed. D. G. Hall, Wiley-VCH, Weinheim, 2nd edn, 2011, vol. 1 and 2.
- (a) J. F. Hartwig, K. S. Cook, M. Hapke, C. D. Incarvito, Y. Fan, C. E. Webster and M. B. Hall, *J. Am. Chem. Soc.*, 2005, **127**, 2538–2552; (b) C. E. Webster, Y. Fan, M. B. Hall, D. Kunz and J. F. Hartwig, *J. Am. Chem. Soc.*, 2003, **125**, 858–859.
- (a) A. Ros, R. Fernández and J. M. Lassaletta, *Chem. Soc. Rev.*, 2014, **43**, 3229–3243; (b) J. F. Hartwig, *Acc. Chem. Res.*, 2012, **45**, 864–872; (c) J. F. Hartwig, *Chem. Soc. Rev.*, 2011, **40**, 1992–2002; (d) I. A. I. Mkhalid, J. H. Barnard, T. B. Marder, J. M. Murphy and J. F. Hartwig, *Chem. Rev.*, 2010, **110**, 890–931; (e) T. Ishiyama and N. Miyaura, *J. Organomet. Chem.*, 2003, **680**, 3–11.
- (a) C. M. Kelly, J. T. Fuller III, C. M. Macaulay, R. McDonald, M. J. Ferguson, S. M. Bischof, O. L. Sydora, D. H. Ess, M. Stradiotto and L. Turculet, *Angew. Chem., Int. Ed.*, 2017, **56**, 6312–6316; (b) T. Furukawa, M. Tobisu and N. Chatani, *Bull. Chem. Soc. Jpn.*, 2017, **90**, 332–342; (c) T. Furukawa, M. Tobisu and N. Chatani, *J. Am. Chem. Soc.*, 2015, **137**, 12211–12214.
- (a) M. A. Esteruelas, A. M. López and M. Oliván, *Chem. Rev.*, 2016, **116**, 8770–8847; (b) I. M. Riddlestone, J. A. B. Abdalla and S. Aldridge, *Adv. Organomet. Chem.*, 2015, **63**, 1–38; (c) G. Alcaraz, M. Grellier and S. Sabo-Etienne, *Acc. Chem. Res.*, 2009, **42**, 1640–1649; (d) Z. Lin, *Transition Metal  $\sigma$ -borane complexes*, in *Contemporary metal boron chemistry I: borylenes, boryls, borane  $\sigma$ -complexes and borohydrides*, ed. T. B. Marder and Z. Lin, Springer, 2008, vol. 130, pp. 123–148.
- (a) A. Cassen, Y. Gloaguen, L. Vendier, C. Duhayon, A. Poblador-Bahamonde, C. Raynaud, E. Clot, G. Alcaraz and S. Sabo-Etienne, *Angew. Chem., Int. Ed.*, 2014, **53**, 7569–7573; (b) C. Y. Tang, A. L. Thompson and S. Aldridge, *J. Am. Chem. Soc.*, 2010, **132**, 10578–10591.
- (a) M. Roselló-Merino, R. J. Rama, J. Díez and S. Conejero, *Chem. Commun.*, 2016, **52**, 8389–8392; (b) M. Roselló-Merino, J. López-Serrano and S. Conejero, *J. Am. Chem. Soc.*, 2013, **135**, 10910–10913.
- P. Ríos, H. Fouilloux, P. Vidossich, J. Díez, A. Lledós and S. Conejero, *Angew. Chem., Int. Ed.*, 2018, **57**, 3217–3221.
- M. Brookhart, M. L. H. Green and G. Parkin, *Proc. Natl. Acad. Sci. U. S. A.*, 2007, **104**, 6908–6914.
- (a) H. Braunschweig, K. Radacki and K. Uttinger, *Chem.–Eur. J.*, 2008, **14**, 7858–7866; (b) H. Braunschweig, P. Brenner, A. Müller, K. Radacki, D. Rais and K. Uttinger, *Chem.–Eur. J.*, 2007, **13**, 7171–7176; (c) H. Braunschweig, K. Radacki, D. Rais and D. Scheschkewitz, *Angew. Chem., Int. Ed.*, 2005, **44**, 5651–5654.
- G. Alcaraz and S. Sabo-Etienne, *Coord. Chem. Rev.*, 2008, **252**, 2395–2409.
- (a) J. C. Babón, M. A. Esteruelas, I. Fernández, A. M. López and E. Oñate, *Inorg. Chem.*, 2018, **57**, 4482–4491; (b) M. A. Esteruelas, I. Fernández, C. García-Yebra, J. Martín and E. Oñate, *Organometallics*, 2017, **36**, 2298–2307; (c) K. K. Pandey, *Inorg. Chem. Commun.*, 2008, **11**, 288–292.
- (a) A. Kumar, N. A. Beattie, S. D. Pike, S. A. Macgregor and A. S. Weller, *Angew. Chem., Int. Ed.*, 2016, **55**, 6651–6656; (b) M. C. MacInnis, R. McDonald, M. J. Ferguson, S. Tobisch and L. Turculet, *J. Am. Chem. Soc.*, 2011, **133**, 13622–13633; (c) G. Alcaraz, L. Vendier, E. Clot and S. Sabo-Etienne, *Angew. Chem., Int. Ed.*, 2010, **49**, 918–920; (d) C. Y. Tang, A. L. Thompson and S. Aldridge, *Angew. Chem., Int. Ed.*, 2010, **49**, 921–925.
- K. K. Pandey, *J. Mol. Struct.: THEOCHEM*, 2008, **855**, 18–26.
- Different functionals and basis sets have been employed in these calculations, and no BCP between B and Pt has been observed in any case (see ESI† for more details).



- 17 (a) H. Braunschweig, K. Kraft, T. Kupfer and E. Siedler, *Z. Anorg. Allg. Chem.*, 2010, **636**, 2565–2567; (b) T. J. Hebden, M. C. Denney, V. Pons, P. M. B. Piccoli, T. F. Koetzle, A. J. Schultz, W. Kaminsky, K. I. Goldberg and D. M. Heinekey, *J. Am. Chem. Soc.*, 2008, **130**, 10812–10820; (c) M. G. Crestani, M. Muñoz-Hernández, A. Arévalo, A. Acosta-Ramírez and J. J. García, *J. Am. Chem. Soc.*, 2005, **127**, 18066–18073; (d) V. Montiel-Palma, M. Lumbierres, B. Donnadieu, S. Sabo-Etienne and B. Chaudret, *J. Am. Chem. Soc.*, 2002, **124**, 5624–5625; (e) S. Schlecht and J. F. Hartwig, *J. Am. Chem. Soc.*, 2000, **122**, 9435–9443; (f) J. F. Hartwig, C. N. Muhoro and X. He, *J. Am. Chem. Soc.*, 1996, **118**, 10936–10937.
- 18 G. Sciortino, A. Lledós and P. Vidossich, *Dalton Trans.*, 2019, **48**, 15740–15752.
- 19 P. Ríos, H. Fouilloux, J. Díez, P. Vidossich, A. Lledós and S. Conejero, *Chem.–Eur. J.*, 2019, **25**, 11346–11355.
- 20 Likely, a dynamic low energy barrier process (4.9 kcal mol<sup>-1</sup> from **4a** to **Int2**; see Figure 6) involving de-coordination/coordination of the O atom from platinum is responsible for the NMR equivalence of these CH<sub>2</sub> protons.
- 21 M. Ortuño, S. Conejero and A. Lledós, *Beilstein J. Org. Chem.*, 2013, **9**, 1352–1382.
- 22 For some examples of reversible C–B bond formation processes in organoboron compounds see: (a) Z.-C. He, S. K. Møllerup, L. Liu, X. Wang, C. Dao and S. Wang, *Angew. Chem., Int. Ed.*, 2019, **58**, 6683–6687; (b) S. K. Møllerup, C. Li, X. Wang and S. Wang, *J. Org. Chem.*, 2018, **83**, 11970–11977; (c) A. F. Eichhorn, S. Fuchs, M. Flock, T. B. Marder and U. Radius, *Angew. Chem., Int. Ed.*, 2017, **56**, 10209–10213; (d) B. E. Cowie and D. J. H. Emslie, *Organometallics*, 2015, **34**, 2737–2746; (e) D.-T. Yang, S. K. Møllerup, X. Wang, J.-S. Lu and S. Wang, *Angew. Chem., Int. Ed.*, 2015, **56**, 5498–5501.
- 23 G. C. Fortman, N. M. Scott, A. Linden, E. D. Stevens, R. Dorta and S. P. Nolan, *Chem. Commun.*, 2010, **46**, 1050–1052.
- 24 O. Rivada-Wheelaghan, M. Roselló-Merino, M. A. Ortuño, P. Vidossich, E. Gutiérrez-Puebla, A. Lledós and S. Conejero, *Inorg. Chem.*, 2014, **53**, 4257–4268.
- 25 M. A. Ortuño, P. Vidossich, S. Conejero and A. Lledós, *Angew. Chem., Int. Ed.*, 2014, **53**, 14158–14161.
- 26 R. N. Perutz and S. Sabo-Etienne, *Angew. Chem., Int. Ed.*, 2007, **46**, 2578–2592.
- 27 (a) D. Franz and S. Inoue, *Chem.–Eur. J.*, 2019, **25**, 2898–2926; (b) W. E. Piers, S. C. Bourke and K. D. Conroy, *Angew. Chem., Int. Ed.*, 2005, **44**, 5016–5036.

